Provisional chapter

Dye-Linked Flavin-Containing Dehydrogenase from Bacteria Related to Plant

Seiya Watanabe

Additional information is available at the end of the chapter

Abstract

The so-called dye-linked dehydrogenases catalyze the oxidation of various biomolecules in the presence of an artificial electron acceptor, in which several unique compounds related to plants as substrates such as opine(s) and L-hydroxyproline are contained. Opines including nopaline and octopine are produced from nutrients of plant by pathogenic agrobacteria species in a crown gall tumor and subsequently degraded for their nutrients by (hypothetical) opine dehydrogenase(s) (OpnDH). The homologous proteins of *Pseudomonas putida* and *Bradyrhizobium japonicum* (isozymes 1 and 2) function as nopaline- and octopine-specific dye-linked dehydrogenases, to yield α-ketoglutarate + L-arginine and pyruvate + L-arginine, respectively. L-Hydroxyproline is detected in such hydroxyproline-rich glycoprotein of plant cell walls. In the degradation pathway of bacteria, D-hydroxyproline dehydrogenase (HypDH) catalyzes the dehydrogenation reaction of *cis*-4-hydroxy-D-proline, and is classified into two types: homomeric and heteromeric enzymes. Both OpnDH and heteromeric HypDH commonly consist of three different subunits ($\alpha\beta\gamma$), in which 2 FAD, 1 FMN, [2Fe-2S] and [4Fe-4S] clusters are contained as prosthetic groups. In D-amino acid dehydrogenase superfamily, these enzymes are physiologically related to L-proline dehydrogenase from archaea and hydrogen cyanide synthase from bacteria, whereas isozyme 2 of OpnDH from *B. japonicum* and other OpnDHs had appeared by convergent evolution.

Keywords: dye-linked dehydrogenase, opine, L-hydroxyproline, molecular evolution

1. Introduction

Oxidoreductases catalyze the reversible electron-transfer from many compounds such as amino acids, alcohols, sugars, and amines, and are classified into three main groups, based on available

electron acceptor(s): oxidases, oxygenases and dehydrogenases/reductases. FAD- and/or FMN-dependent dehydrogenases, one of subgroups in dehydrogenases/reductases, play a variety of important roles in the generation of energy and in the biosynthesis and metabolism of biomolecules [1, 2]. These enzymes are frequently called as "dye-linked dehydrogenases", because of utilization of artificial dyes such as 2,6-dichloroindophenol (Cl2Ind) and ferricyanide instead of the natural acceptor(s). Furthermore, most of them are frequently associated with cell or organelle membranes and are unstable in solution, which has made their expression in host cells, purification, preservation, and characterization very difficult. Since dye-linked dehydrogenation activity for several unique compounds related to plants as substrates including opine(s) and L-hydroxyproline had been reported in bacterial cell-free extract from 1950s to 1980s, those genetic and molecular information have only recently been elucidated [3–6].

2. Opine dehydrogenase

2.1. Opine concept

Plant tumors known as crown gall are incited by pathogenic, soil-inhabiting *Agrobacterium* species including *Agrobacterium tumefaciens*. During the infections [7], the expression of the virulence genes (*vir*) within the tumor-inducing (Ti) plasmid is first specifically induced by phenolic compounds, including acetosyringone, which are released from the wounded plant cells (① in **Figure 1**). Next, the products expressed by the *virD* locus promote fragmentation of so-called T-DNA region (②) and subsequently transfer to the nuclei of host plants (③). T-DNA region integrated into a host chromosome contains several genes including synthase(s) of phytohormones such as auxin and cytokinin (④), and the genetic expressions direct the production of phytohormones such as auxin and cytokinin, which can lead to uncontrolled cell proliferation, producing a crown gall tumor (⑤). The (integrated) T-DNA region also encodes genes for the synthesis of unique compounds, opines (⑥). The opines produced and secreted by the neoplastic plant cells are utilizable as nutrient sources by the agrobacteria that induced the tumor (⑦). The genes for the utilization of the opines by the bacteria are also encoded by the Ti plasmid, but they are located outside the T-DNA region (⑧) (i.e., the "opine concept").

2.2. What's opine?

Opines have been structurally classified into several groups, among which two groups have a common secondary amine dicarboxylic acid structure. One group has been categorized as the N^2-(L-D-carboxyethyl) derivatives of L-arginine (octopine), L-ornithine (octopinic acid), L-lysine (lysopine), L-histidine (histopine), L-methionine (methiopine), and L-phenylalanine (phenylalaninopine). The second group has been categorized as the N^2-(1,3-D-dicarboxypropyl) derivatives of L-arginine (nopaline), L-ornithine (nopalinic acid (ornaline)), L-leucine (leucinopine), and L-asparagine (succinamopine). Of these, octopine (N^2-(L-D-carboxyethyl) derivatives of L-arginine) and nopaline (N^2-(1,3-D-dicarboxypropyl) derivatives of L-arginine) are

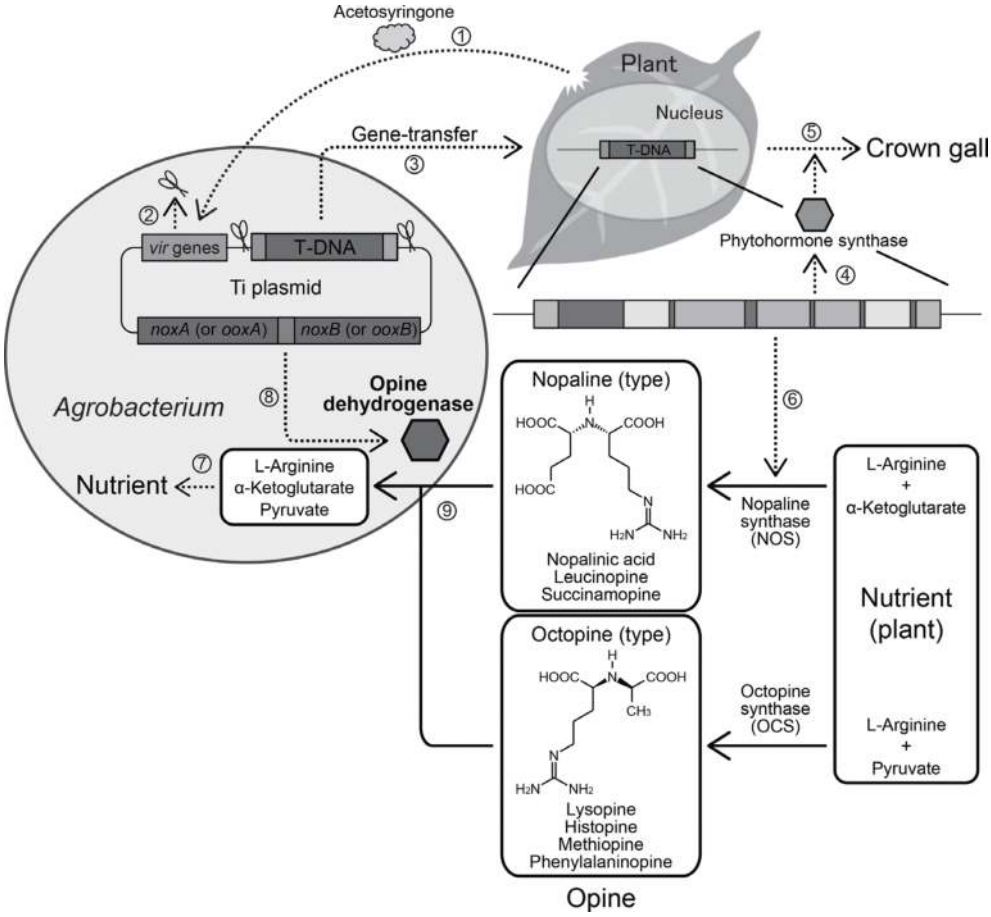

Figure 1. Opine concept by *Agrobacterium*.

well studied, and synthesized by NAD(P)H-dependent soluble dehydrogenases: octopine synthase (OCS; [8]) and nopaline synthase (NOS; [9]) (⑥ in **Figure 1**). These enzymes catalyze the reductive condensation of pyruvate (for octopine) or α-ketoglutarate (for nopaline) with L-arginine. Although these reactions may be reversible *in vitro*, the frequent use of the term "synthase" rather than "dehydrogenase" has emphasized the importance of "biosynthesis", but not "degradation".

2.3. Opine assimilation by *Agrobacterium*

The octopine catabolic (*occ*) operons of octopine-type Ti plasmids consist of at least 15 genes that include ABC-type (opine) permease (encoded by *occQMPJ*) and ornithine cyclodeaminase

(*ocd*) [10] (**Figure 2**). On the other hand, nopaline-metabolizing genes including *nos* are encoded within the nopaline catabolic (*noc*) region in the pTiC58 plasmid [11]. Both the *occ* operon and *noc* region also contain several genes suspected of being involved in opine metabolism such as *ooxA* (pTi_037), *ooxB* (pTi_038), *noxA* (Atu6019), and *noxB* (Atu6021) (**Figure 2A**). In both opines, the first step of degradation is the reverse of biosynthesis, i.e., oxidative cleavage to L-arginine and pyruvate or α-ketoglutarate (⑨ in **Figure 1**): L-arginine may subsequently be metabolized to L-proline via L-ornithine through two sequential enzyme reactions by arginase (encoding *arc*) and ornithine cyclodeaminase. More than 20 years ago, it was reported that when *noxB-noxA* and *ooxB-ooxA* were transcriptionally fused with the vector promoter and expressed in *Escherichia coli* cells, cofactor-independent oxidase activities for nopaline and octopine were observed in the membrane fraction [12]. However, these activities were directly assayed using the *E. coli* lysate with lysozyme (without centrifugation). Until now, there has been no clear evidence to show that these genes (proteins) function as opine oxidases.

2.4. Nopaline dehydrogenase from *Pseudomonas putida*

2.4.1. Successful preparation of recombinant protein

The homologous *ooxB-ooxA* and *noxB-noxA* genes exist as a gene cluster together with putative ABC-type transporter gene(s) on the genomes and/or plasmids of non-*Agrobacterium* bacterial species, although the mechanisms underlying opine catabolism are unclear. Among them, PP_4457 and PP_4456 (genes) from *Pseudomonas putida* KT2440 correspond to OoxB (40% of identity) and NoxB (40%), and OoxA (41%) and NoxA (48%), respectively (referred to as OdhB and OdhA, respectively) (**Figure 2A**). The *odhB-odhA* operon, in which the $(His)_6$-tag sequence

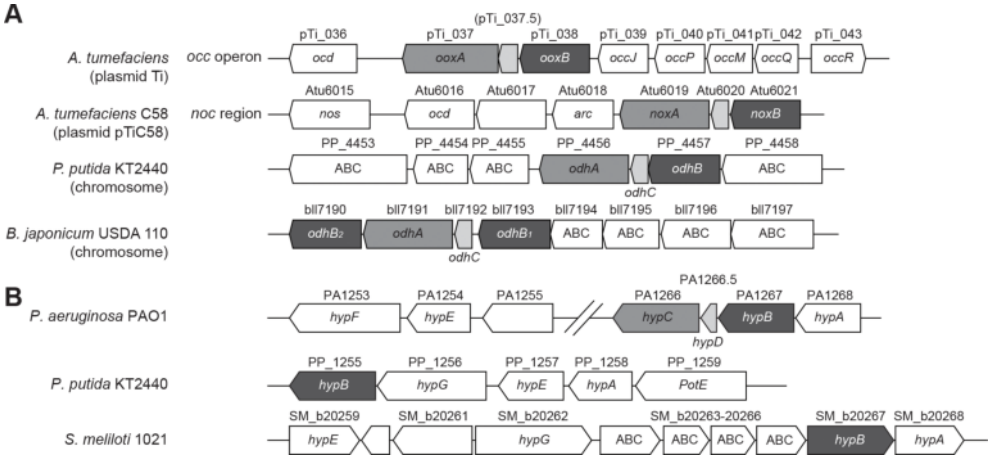

Figure 2. Schematic gene clusters related to opine (A) and L-Hyp metabolism (B).

was attached at the N-terminal of the *odhB* gene, expressed in *P. putida* cell (but not *E. coli*) [13, 14], and purified using immobilized metal (Ni^{2+}) affinity chromatography (**Figure 3A**). A buffer system containing Tween-20 was absolutely necessary for this procedure, indicating tight binding to the cytoplasmic membrane. The purified recombinant protein consisted of three major distinct bands with molecular masses of 46, 42, and 9 kDa, respectively, among which the two formers expectedly corresponded to OdhA and OdhB, respectively. Interestingly, N-terminal sequence of the latter was identical with that of a provisional open-reading frame between *odhA* and *odhB* genes (referred to as *odhC* gene): the 3′ part of *odhB* and *odhC* was slightly overlapped by the 5′ part of *odhC* and *odhA*, respectively. Thus, this protein indeed consisted of α-, β-, and γ-subunits encoded by *odhA*, *odhB*, and *odhC* genes, respectively (referred to as PpOdhABC).

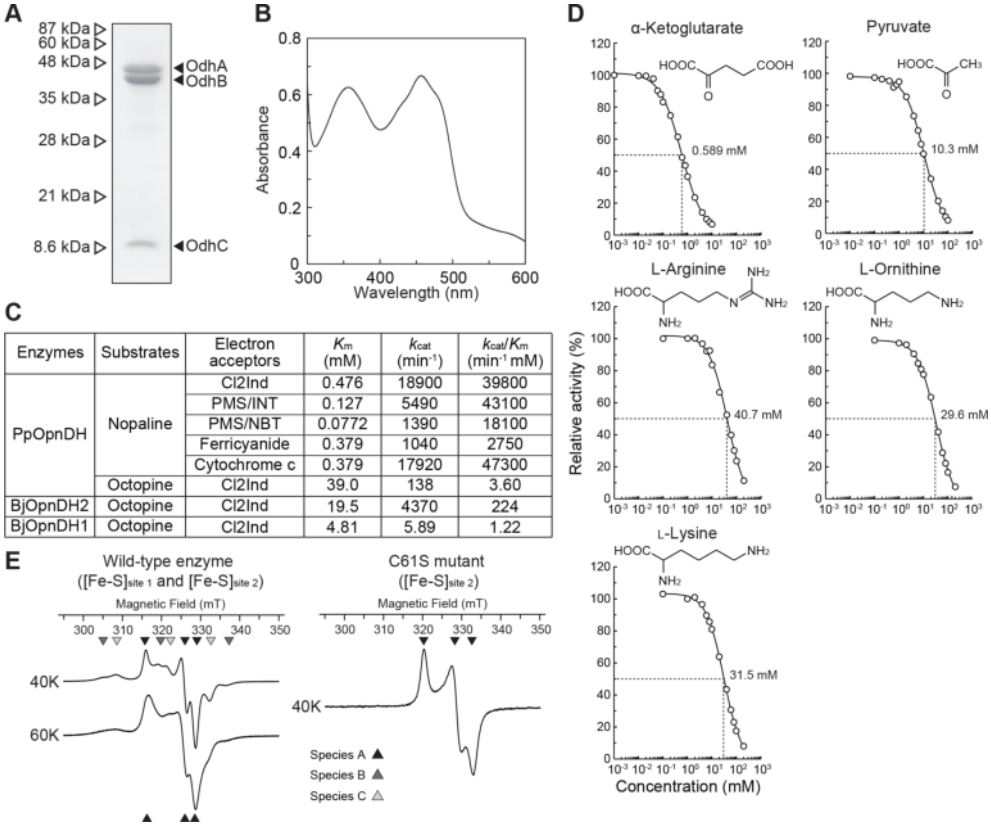

Enzymes	Substrates	Electron acceptors	K_m (mM)	k_{cat} (min^{-1})	k_{cat}/K_m (min^{-1} mM)
PpOpnDH	Nopaline	Cl2Ind	0.476	18900	39800
		PMS/INT	0.127	5490	43100
		PMS/NBT	0.0772	1390	18100
		Ferricyanide	0.379	1040	2750
		Cytochrome c	0.379	17920	47300
	Octopine	Cl2Ind	39.0	138	3.60
BjOpnDH2	Octopine	Cl2Ind	19.5	4370	224
BjOpnDH1	Octopine	Cl2Ind	4.81	5.89	1.22

Figure 3. Characterization of opine dehydrogenase. An SDS-PAGE analysis (A) and absorption spectra (B) of purified recombinant PpOdhABC. (C) Kinetic parameters. (D) Inhibition study by α-keto acids and L-amino acids. (E) EPR spectra of wild-type and C61S (in γ-subunit) of BjOpnDH2.

2.4.2. Prosthetic group(s)

The purified protein was orange-brown, and the absorption spectrum showed the characteristics of a typical flavoprotein (maxima at approximately 350 and 450 nm; **Figure 3A**): the flavin compounds were identified as FAD and FMN by HPLC. Alternatively, each subunit of heteromeric PpOdhABC was also purified and functionally characterized. Only FAD was extracted from (almost) inactive OdhA, OdhB, OdhAB (co-expression of OdhA+B), OdhBC, and OdhAC, while FAD and FMN were only extracted from active OdhABC; the molar ratio of FAD:FMN was 1.9:1.0. Therefore, it was concluded that PpOdhABC contained 2 FAD (α- and β-subunits) and 1 FMN (between the α- and β-subunits) within the structural unit of $\alpha\beta\gamma$ (**Figure 4A**). On the other hand, as described below in detail, the OdhC and OdhA proteins contain two different types of [Fe-S]-binding motifs, in which [4Fe-4S] and [2Fe-2S] clusters might be bound, respectively (see Section 2.6).

2.4.3. Characterization as a dye-linked opine dehydrogenase

When Cl2Ind was used as an artificial electron acceptor, the catalytic efficiency (k_{cat}/K_m) value of PpOdhABC with nopaline was 11,000-fold higher than that with octopine. *p*-Iodonitrotetrazolium violet (INT) or nitroblue tetrazolium (NBT) together with phenazine methosulfate (PMS) (electron-transfer intermediate), ferricyanide, and horse heart cytochrome *c* (but not $NAD(P)^+$ or oxygen) were additional artificial electron acceptors. Since other opines were not available commercially, more detailed substrate specificity was alternatively estimated by an inhibition study (**Figure 4D**). The IC_{50} value for α-ketoglutarate was ~17-fold higher than that for pyruvate, thereby confirming the preference for nopaline over octopine. On the other hand, among several L-amino acids, significant inhibition was only observed in basic L-arginine, L-ornithine, and L-lysine. These results indicated that PpOdhABC recognized the *N*-substituted glutamic acid moiety of nopaline and nopalinic acid (**Figure 1**), also found in crown gall tumor tissues, and may also be the active substrate.

2.5. Octopine dehydrogenase from *Bradyrhizobium japonicum*

Bradyrhizobium japonicum is a nitrogen-fixing bacteria found in the roots of a soybean plant, *Glycine max*. Interestingly, the homologous gene cluster with *odhB-odhC-odhA* from *P. putida* contained an additional *odhB* gene, in the order of *odhB*$_1$-*odhC-odhA-odhB*$_2$ (**Figure 2A**) In order to estimate the subunit assembly of this protein, $(His)_6$-tagged $OdhB_1$ or $OdhB_2$ was co-expressed together with S-tagged OdhA and OdhC in *E. coli* cells and purified using Ni^{2+}-affinity chromatography. A western blotting analysis using the anti $(His)_6$-tag and S-tag antibodies revealed that the purified proteins both contained not only each OdhB, but also OdhA and OdhC (referred to as $BjOdhAB_1C$ and $BjOdhAB_2C$, respectively) (**Figure 4A**).

Their absorption spectra were similar to that of PpOpnDH, and FAD and FMN (the molar ratio of ~2) were extracted from (orange-brown) them. On the other hand, the significant dehydrogenase activities were detected only toward octopine, although the specific activity of $BjOdhAB_1C$ was ~200-fold lower than that of $BjOdhAB_2C$ (**Figure 3C**). The k_{cat}/K_m value for the octopine of $BjOdhAB_2C$ (using Cl2Ind; 224 min^{-1} mM^{-1}) was 178-fold lower than that

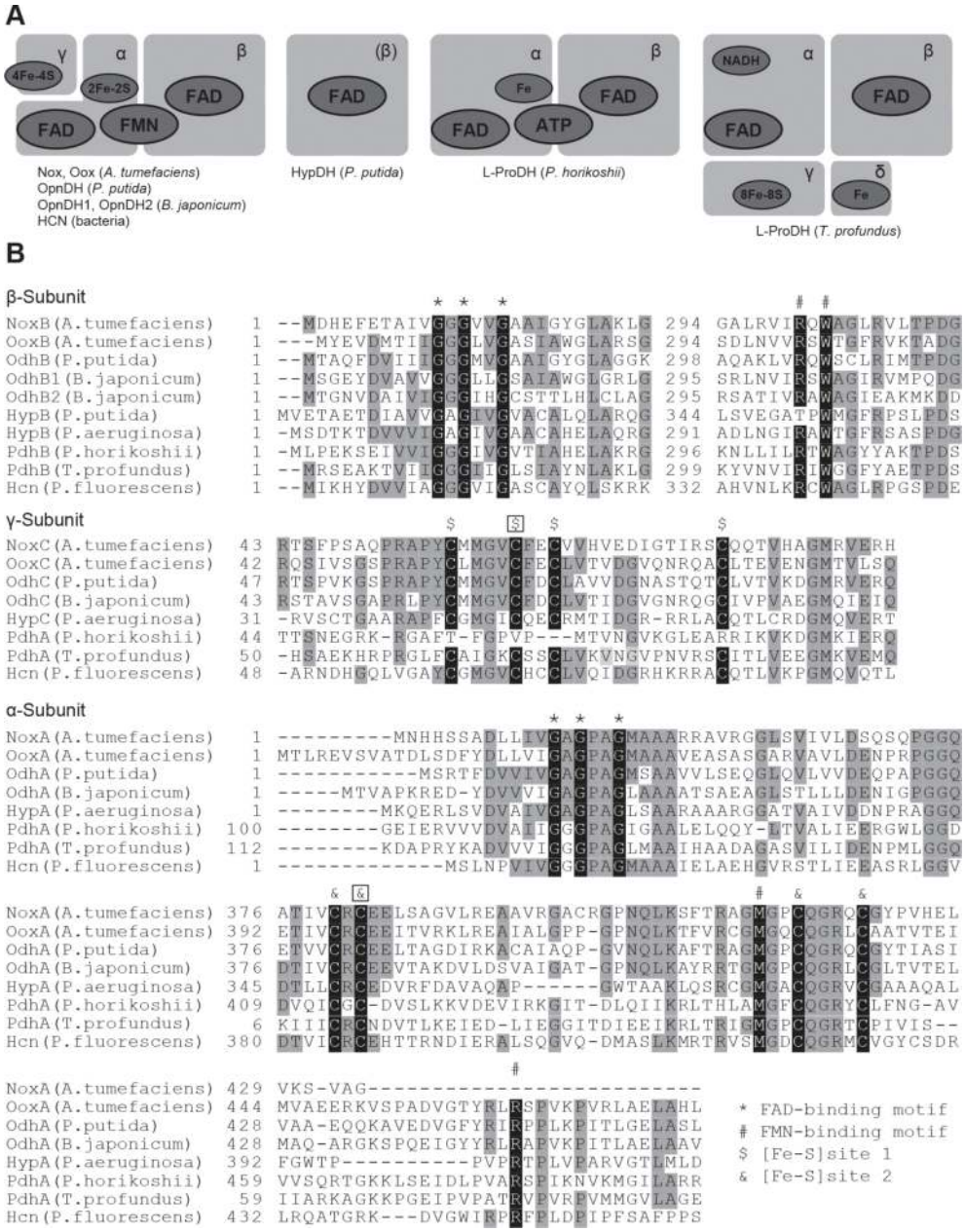

Figure 4. Schematic subunit assembly (A) and partial amino acid sequence alignment of dehydrogenases (B).

for the nopaline of PpOpnDH. These results suggested that BjOdhAB$_2$C and BjOdhAB$_1$C both functioned as octopine-specific OpnDH (referred to as BjOpnDH2 and BjOpnDH1, respectively).

2.6. Functional role(s) of iron-sulfur clusters

The γ- and α-subunits of OpnDH contain two different types of [Fe-S]-binding motifs consisting of four cysteine residues: $[Fe\text{-}S]_{site\ 1}$ and $[Fe\text{-}S]_{site\ 2}$, respectively (**Figure 4B**). An electron paramagnetic resonance (EPR) spectrum recorded for the frozen solution of the BjOpnDH2 wild-type enzyme (fully reduced by $Na_2S_2O_4$) at 40 K was composed of at least three paramagnetic species due to [Fe-S] clusters: species A, B, and C (**Figure 3E**). Among them, only species A was still detected at 60 K, indicating the assignment to be the fully reduced form of $[2Fe\text{-}2S]^-$ (therefore, species B and C were derived from the reduced form of $[4Fe\text{-}4S]^{3-}$). On the other hand, when one cysteine residue (Cys^{61}; boxed in **Figure 4B**) in $[Fe\text{-}S]_{site\ 1}$ was substituted to serine residue, the C61S mutant protein showed the significant activity, and the paramagnetic species was clearly similar to species A found in the wild-type enzyme (**Figure 3E**). No expression of C382S mutant in $[Fe\text{-}S]_{site\ 2}$ was found in *E. coli* (**Figure 4B**). Wholly, $[Fe\text{-}S]_{site\ 1}$ and $[Fe\text{-}S]_{site\ 2}$ of heteromeric OpnDH bind to the [4Fe-4S] and [2Fe-2S] clusters, respectively (**Figure 4A**), and the latter is important for structural folding and enzyme catalysis.

2.7. Phylogenetic relationship

Flavin-containing OpnDH (the β-subunit) belongs to the D-amino acid oxidase superfamily (pfam01266), and differed from the known $NAD(P)^+$-dependent enzyme (pfam02317) [8, 9]. Although this protein superfamily contains several oxidases for D-amino acid and sarcosine, a relatively high homology with OpnDH was found in hydrogen cyanide (HCN) synthase from bacteria [15], D-hydroxyproline dehydrogenase (HypDH) from bacteria (described in Section 3; [4]), and L-proline dehydrogenase (L-ProDH) from archaea with a heterooligomeric structure [16] (**Figure 5A**). The subunit assembly of OpnDH (αβγ) was the same as that of HypDH and HCN synthase (**Figure 4A**). PpOpnDH and BjOpnDH1 formed a single subfamily together with Nox and Oox from *A. tumefaciens* (referred to as the $OpnDH_{type\ 1}$ subfamily). Interestingly, BjOpnDH2 was not closely related to any of the subclasses including $OpnDH_{type\ 1}$

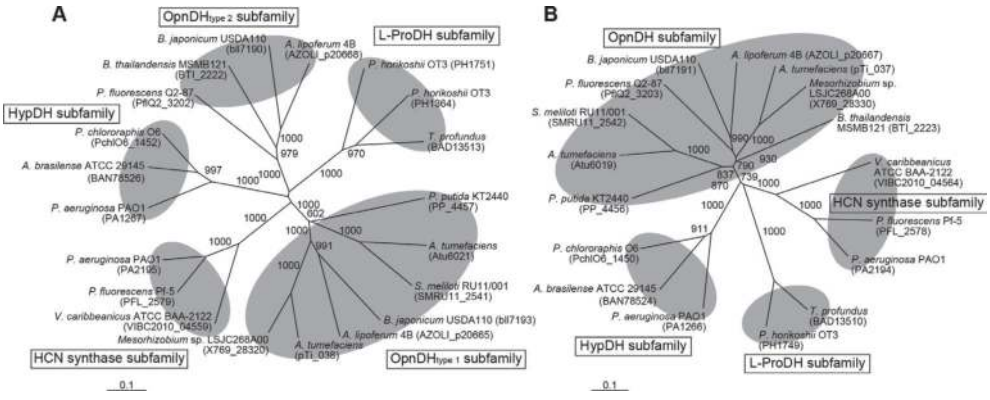

Figure 5. Phylogenetic trees using β- (A) and α-subunits (B) of flavin-containing dye-linked dehydrogenases.

(referred to as $OpnDH_{type\ 2}$ subfamily) (**Figure 5A**), whereas all OdhA proteins formed a single subfamily (**Figure 5B**). Several specific motifs (amino acid residues), previously proposed in L-ProDHs, are significantly conserved in the primary structure(s) of OpnDH: two typical ADP-binding motifs at the N-terminus of the β- and α-subunits as (putative) the binding sites of 2 FAD (Gly-*X*-Gly-X_2-Gly); a motif of Arg-*X*-Trp for (putative) the binding sites of FMN in the α-subunit (and β-subunit) (**Figure 4B**).

2.8. Physiological role

The degradation of toxic organic compounds by some *P. putida* strains has been extensively examined [17]. On the other hand, these bacteria, in addition to *B. japonicum*, also colonize the rhizosphere of agronomically relevant plants at high population densities; the origin of opines may be from rotting plants and/or plant exudates rather than biosynthesis. In case of endophytes, opines may be also provided without their being exuded. It is reported that a *P. putida* strain isolated from a commercial nursery catabolized nopaline [18], thereby conforming to the substrate specificity of PpOpnDH. In contrast to *Agrobacterium* species, PpOpnDH and BjOpnDH genes are located on the chromosome. Indeed, large numbers of *Bradyrhizobium* species possess the homologous genes, whereas all the other *P. putida* strains, except for KT2440, do not. These findings suggest that *P. putida* KT2440 very recently acquired this ability by horizontal gene transfer (not plasmid transfer).

3. D-Hydroxyproline dehydrogenase

3.1. L-Hydroxyproline in nature

trans-4-Hydroxy-L-proline (T4LHyp; generally called "L-hydroxyproline (L-Hyp)") is a non-standard amino acid, and detected in certain proteins including collagen, the cell wall of plants, and some peptide antibiotics. In the two former proteins, L-proline residue is post-translationally hydroxylated to L-Hyp by α-ketoglutarate and Fe(II)-dependent prolyl hydroxylase (① and ② in **Figure 6**). In case of so-called "hydroxyproline-rich glycoprotein (HRGP)" of plant cell walls including extensins and solanaceous lectins, Hyp-residues are subsequently glycosylated by hydroxyproline *O*-arabinosyltransferase (③) [19]. The β-L-arabinofuranoside (Ara)-containing HPRGs have repetitive Ser-Hyp_4 motifs and the majority of the Hyp-*O*-linked arabinofuranosides are Ara-Ara-Ara-Ara-Hyp and Ara-Ara-Ara-Hyp. In degradation system of the latter by bacteria such as *Bifidobacterium longum*, two β-L-arabinobiosidases HypBA2 and HypBA1 release Ara-Ara from Ara_3-Hyp (④), and subsequently liberate Ara from Ara-Ara, respectively (⑤), although no enzyme degrading Ara-Hyp to Ara and L-Hyp is known until now (⑥) and this bacterium may have no ability to metabolize L-Hyp by itself [20]. On the other hand, direct biosynthesis from free L-proline to L-Hyp by hydroxylase(s) from few bacteria (and fungi) such as *Streptomyces* sp. may be in the biosynthesis of peptide antibiotics containing L-Hyp such as etamycin (⑦) [21]. Therefore, free L-Hyp may also be produced by the degradation of these proteins and/or antibiotics through protease (peptidase), particularly in soil and water environments (⑧).

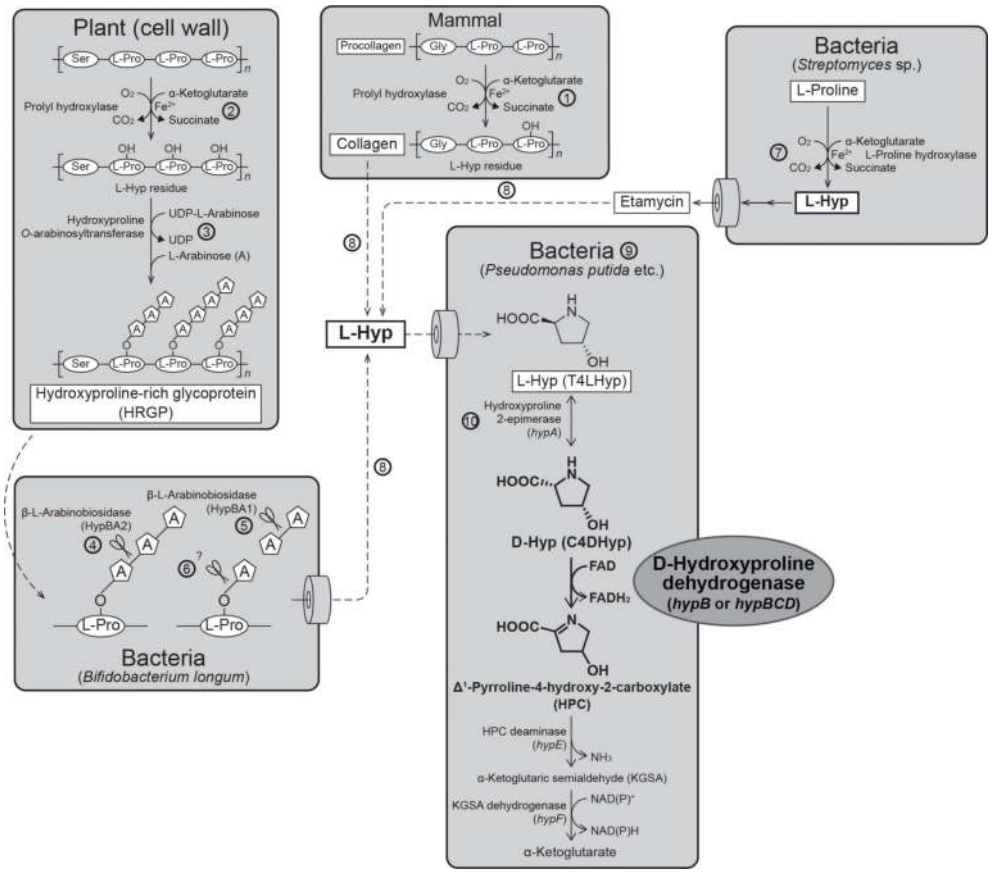

Figure 6. A hypothetical schematic between L-Hyp and organisms in nature.

3.2. Involvement in bacterial L-Hyp pathway

In contrast to mammals, bacteria metabolize free T4LHyp to α-ketoglutarate through four enzymatic steps via *cis*-4-hydroxy-D-proline (C4DHyp; generally called "D-hydroxyproline"), Δ^1-pyrroline-4-hydroxy-2-carboxylate, and α-ketoglutaric semialdehyde intermediates (⑨); therefore, bacteria with this pathway have the ability to grow using not only T4LHyp, but also C4DHyp as the sole carbon source. D-Hydroxyproline dehydrogenase (HypDH) catalyzes the dehydrogenation reaction of C4DHyp to Δ^1-pyrroline-4-hydroxy-2-carboxylate (second step of bacterial T4LHyp pathway): C4DHyp is produced from T4LHyp by hydroxyproline 2-epimerase (⑩). More than 40 years ago, it had been already known that the enzyme has the ability to utilize artificial electron acceptors including Cl2Ind as well as OpnDH, but there was no genetic report until now, probably because of the dye-linked dehydrogenase, as described in "Introduction" [22]. On the other hand, the genes (*hypA~hypF*) related to (putative) T4LHyp pathway are often clustered together with those encoding the transporter on bacterial genomes (referred to as T4LHyp gene cluster) (**Figure 2B**).

3.3. Homomeric HypDH

Among T4LHyp gene clusters of *P. putida* KT2440 and (nitrogen-fixing) *Sinorhizobium meliloti* 2011, PP_1255 and SM_b20267 genes, annotated as FAD-dependent oxidoreductase and D-amino acid dehydrogenase, respectively, were likely candidates for HypDH (referred to as *PphypB* and *SmhypB*, respectively) (**Figure 2B**). When *E. coli* (even *S. meliloti*) was used as a host, no expression of these recombinant proteins was found probably due to the membrane bound and dye-linked dehydrogenase as well as OpnDH: their biochemical characterizations were achieved by the same expression and purification systems as PpOpnDH (**Figure 7A**). Spectra of both the purified HypB proteins commonly showed the characteristics of a typical flavoprotein (**Figure 7B**), and only FAD was contained as a prosthetic group. Among several tested D-amino acids, their significant activities were observed only with C4DHyp and D-proline (referred to as PpHypDH and SmHypDH). The k_{cat}/K_m value with C4DHyp of PpHypDH

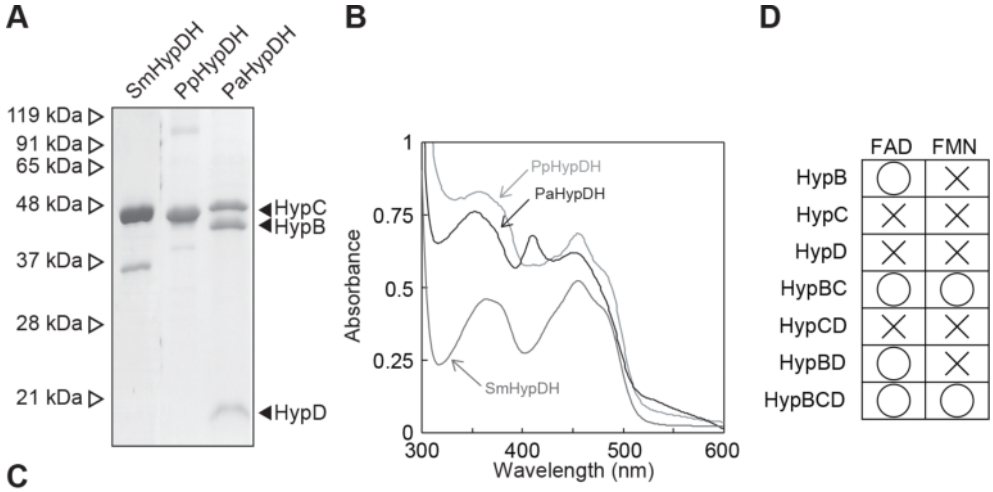

C

Enzymes	Substrates	Electron acceptors	K_m (mM)	k_{cat} (min^{-1})	k_{cat}/K_m (min^{-1} mM)	C4DHyp / D-Proline
PpHypDH	C4DHyp	PMS/INT	0.276	280	1010	110
		PMS/NBT	0.0802	19.7	246	
	D-Proline	PMS/INT	6.58	59.9	9.15	
		PMS/NBT	3.49	9.95	2.86	
SmHypDH	C4DHyp	PMS/INT	0.188	125	665	5.5
		PMS/NBT	0.0602	61.0	1014	
	D-Proline	PMS/INT	0.942	115	122	
		PMS/NBT	0.401	67.4	169	
PaHypDH	C4DHyp	PMS/INT	0.109	2230	20500	190
		PMS/NBT	0.121	871	7200	
	D-Proline	PMS/INT	8.55	924	108	
		PMS/NBT	11.0	507	46.0	

Figure 7. Characterization of D-hydroxyproline dehydrogenase. An SDS-PAGE analysis (A) and absorption spectra (B) of purified recombinant HypDHs. (C) Kinetic parameters. (D) Functional characterization of α- (HypC), β- (HypB), and γ-subunits (HypC).

was 190-fold higher than that with D-proline, mainly caused by much lower K_m value. Only PMS/INT and PMS/NBT (but not Cl2Ind, ferricyanide, cytochrome *c* and $NAD(P)^+$) were available electron acceptor (**Figure 7C**). On the other hand, a ratio of C4DHyp to D-proline in k_{cat}/K_m of SmHypB was only 5.5.

3.4. Heteromeric HypDH

When compared with *P. putida* and *S. meliloti*, T4LHyp gene cluster of *Pseudomonas aeruginosa* PAO1 contained several additional genes, PA1267 (glycine/D-amino acid oxidase; *hypB*), PA1266 (heterotetrameric sarcosine oxidase α-subunit; *hypC*), and PA1266.5 (ferredoxin; *hypD*), in the order of *hypB-hypD-hypC* (**Figure 2B**). The *hypB-hypD-hypC* operon, in which the $(His)_6$-tag sequence was attached at the N-terminal of the *hypB* gene, was also expressed in *P. putida* cells (but not *E. coli*), and the recombinant protein was successfully purified to homogeneity. On SDS-PAGE analysis, three distinct bands with the estimated molecular mass of 48, 42 and 10 kDa were observed and corresponded to HypC (α-subunit), HypB (β), and HypD (γ) by LC-ESI-MS/MS analysis, respectively (**Figure 7A**). When compared with PpHypDH, this protein has similar specificity for C4DHyp and electron acceptor availability (referred to as PaHypDH). On the other hand, the k_{cat}/K_m value with C4DHyp was ~20-fold higher than that of PpHypDH probably due to the high stability (**Figure 7C**).

In contrast to homomeric HypDHs, both FAD and FMN (the molar ratio of ~2) were detected as prosthetic groups as well as OpnDH. On the other hand, when each subunit was functionally characterized, only proteins containing the HypB were active (**Figure 7D**). Only FAD was extracted from HypB (~0.8 mol/mol of protein), while FAD and FMN were extracted from HypBC (and HypBCD). These indicated that the dehydrogenation activity of heteromeric HypDH dependents only to β-subunit, and that the γ-subunit had no effect on the binding of FMN. Since two [Fe-S]-binding sites in the γ- and α-subunits were conserved, this enzyme might also contain [4Fe-4S] and [2Fe-2S] clusters as well as OpnDH (see Section 2.6) (**Figure 4A**).

3.5. Comparison with archaeal L-proline dehydrogenases

In spite of their same functions, there is only ~20% of sequence similarity of PpHypDH to PaHypDH (β-subunit) in D-amino acid oxidase superfamily. On the other hand, PaHypDH shows high sequential similarities to two dye-linked L-ProDHs from archaea (and OpnDH and HCN synthase) with heteromeric structure (**Figures 4** and **5**). First, L-ProDH of *Thermococcus profundus* is heterotetrameric structure of αβγδ containing 2 FAD (in α- and β-subunits) [23]. Second, L-ProDH (isozyme 1) of *Pyrococcus horikoshii* is heterooctameric structure of $\alpha_4\beta_4$ containing 1 FAD (β), 1 FMN (between α- and β-subunits), and 1 ATP (α) [24]. The γ-subunit of HypDH (and OpnDH and HCN synthase) corresponds to the N-terminal ~120 amino acid residues of the α-subunit of these L-ProDHs. Since the β-subunits show dehydrogenation activity by themselves, this subunit functionally corresponds to homomeric enzymes: so-called catalytic subunit [3, 5, 23]. On the other hand, the α-subunits may contribute to the regulation of catalysis, because of the binding of several prosthetic group(s) including FAD, ATP, Fe,

and/or NADH (**Figure 4B**). In fact, the heteromeric subunit assembly of HypDH significantly increases catalysis: 39-fold higher k_{cat}/K_m value for C4DHyp than that of the β-subunit alone due to 21-fold lower K_m value [3, 5].

3.6. Physiological role

It was believed that HypDH is involved only in T4LHyp but not in proline metabolism. In case of *S. meliloti*, the *hypB* mutant continues to grow on T4LHyp, but at half the wild-type rate, which may be due to alternative D-amino acid oxidases with broad specificity [25]. In fact, Rmar_0499 protein from *Rhodothermus marinus* JCM9785, whose gene is located within T4LHyp metabolic gene cluster, shows dehydrogenation activity not only toward C4DHyp but also several D-amino acids including (the most preferable) D-phenylalanine [1, 2]. Furthermore, the disruption of *hypB* also leads to a significant decrease of growth on D-proline. Since a ratio of C4DHyp to D-proline in k_{cat}/K_m of SmHypB is significantly low compared with those of PpHypDH and PaHypDH [3], this enzyme must physiologically function as a D-proline dehydrogenase in D-proline metabolism.

In addition to T4LHyp, other relatively rare L-Hyp compounds such as *cis*-4-hydroxy-L-proline (C4LHyp), *trans*-3-hydroxy-L-proline (T3LHyp), and *cis*-3-hydroxy-L-proline (C3LHyp) are found in nature. Among them, genetic and molecular information of T3LHyp and C3LHyp degradation has only recently been elucidated [26–28]. Interestingly, these metabolic genes are often contained within T4LHyp gene cluster on genomes of *S. meliloti* and *P. aeruginosa*, but not *P. putida*. Therefore, it is possible that each L-Hyp gene cluster may be responsible for the metabolism of L-Hyp(s) produced from different natural sources; collagen (containing only T4LHyp and T3LHyp), HRGP (only T4LHyp), and peptide antibiotics (T4LHyp, C4DHyp, C4LHyp, T3LHyp, and/or C3LHyp) (**Figure 6**). In fact, collagenase, peptidase, and/or the peptidase gene are located (closely) within the L-Hyp gene cluster of several bacteria. In addition to (homomeric and heteromeric) HypDH, among metabolic enzymes involved in these L-Hyp pathways, there are several examples of convergent evolution. In different bacterial species, these enzymes are involved in L-Hyp pathways with several combinations, suggesting that even the same L-Hyp pathway(s) evolved independently, at least partially.

Author details

Seiya Watanabe[1,2]*

*Address all correspondence to: irab@agr.ehime-u.ac.jp

1 Department of Bioscience, Graduate School of Agriculture, Ehime University, Matsuyama, Ehime, Japan

2 Faculty of Agriculture, Ehime University, Matsuyama, Ehime, Japan

References

[1] Satomura T, Ishikura M, Koyanagi T, Sakuraba H, Ohshima T, Suye S. Dye-linked D-amino acid dehydrogenase from the thermophilic bacterium *Rhodothermus marinus* JCM9785: Characteristics and role in *trans*-4-hydroxy-L-proline catabolism. Applied Microbiology and Biotechnology. 2015;**99**:4265-4275. DOI: 10.1007/s00253-014-6263-9

[2] Satomura T, Sakuraba H, Suye S, Ohshima T. Dye-linked D-amino acid dehydrogenases: Biochemical characteristics and applications in biotechnology. Applied Microbiology and Biotechnology. 2015;**99**:9337-9347. DOI: 10.1007/s00253-015-6944-z

[3] Watanabe S, Hiraoka Y, Endo S, Tanimoto Y, Tozawa Y, Watanabe Y. An enzymatic method to estimate the content of L-hydroxyproline. Journal of Biotechnology. 2015;**199**:9-16. DOI: 10.1016/j.jbiotec.2015.01.026

[4] Watanabe S, Morimoto D, Fukumori F, Shinomiya H, Nishiwaki H, Kawano-Kawada M, Sasai Y, Tozawa Y, Watanabe Y. Identification and characterization of D-hydroxyproline dehydrogenase and Δ^1-pyrroline-4-hydroxy-2-carboxylate deaminase involved in novel L-hydroxyproline metabolism of bacteria: Metabolic convergent evolution. Journal of Biological Chemistry. 2012;**287**:32674-32688. DOI: 10.1074/jbc.M112.374272

[5] Watanabe S, Sueda R, Fukumori F, Watanabe Y. Characterization of flavin-containing opine dehydrogenase from bacteria. PLoS One. 2015;**10**:e0138434. DOI: 10.1371/journal.pone.0138434. eCollection 2015

[6] Watanabe S, Morimoto D, Fukumori F, Watanabe Y. Characterization of *cis*-4-hydroxyproline dehydrogenase from *Sinorhizobium meliloti*. Bioscience, Biotechnology, and Biochemistry. 2018;**82**:110-113. DOI: 10.1080/09168451.2017.1403887

[7] Bevan MW, Chilton MD. T-DNA of the agrobacterium Ti and Ri plasmids. Annual Review of Genetics. 1982;**16**:357-384

[8] Hack E, Kemp JD. Purification and characterization of the crown gall-specific enzyme, octopine synthase. Plant Physiology. 1980;**65**:949-955

[9] Kemp JD, Sutton DW, Hack E. Purification and characterization of the crown gall specific enzyme nopaline synthase. Biochemistry. 1979;**18**:3755-3760

[10] Flores-Mireles AL, Eberhard A, Winans SC. *Agrobacterium tumefaciens* can obtain sulphur from an opine that is synthesized by octopine synthase using S-methylmethionine as a substrate. Molecular Microbiology. 2012;**84**:845-856. DOI: 10.1111/j.1365-2958.2012.08061.x

[11] Sans N, Schröder G, Schröder J. The Noc region of Ti plasmid C58 codes for arginase and ornithine cyclodeaminase. European Journal of Biochemistry. 1987;**167**:81-87. DOI: 10.1111/j.1432-1033.1987.tb13306.x

[12] Zanker H, Lurz G, Langridge U, Langridge P, Kreusch D, Schröder J. Octopine and nopaline oxidases from Ti plasmids of *Agrobacterium tumefaciens*: Molecular analysis,

relationship, and functional characterization. Journal of Bacteriology. 1994;**176**:4511-4517. DOI: 10.1128/jb.176.15.4511-4517.1994

[13] Hishinuma S, Yuki M, Fujimura M, Fukumori F. OxyR regulated the expression of two major catalases, KatA and KatB, along with peroxiredoxin, AhpC in *Pseudomonas putida*. Environmental Microbiology. 2006;**8**:2115-2124. DOI: 10.1111/j.1462-2920.2006.01088.x

[14] Kobayashi Y, Ohtsu I, Fujimura M, Fukumori F. A mutation in *dnaK* causes stabilization of the heat shock sigma factor σ^{32}, accumulation of heat shock proteins and increase in toluene-resistance in *Pseudomonas putida*. Environmental Microbiology. 2011;**13**:2007-2017. DOI: 10.1111/j.1462-2920.2010.02344.x

[15] Laville J, Blumer C, Von Schroetter C, Gaia V, Défago G, Keel C, Haas D. Characterization of the *hcnABC* gene cluster encoding hydrogen cyanide synthase and anaerobic regulation by ANR in the strictly aerobic biocontrol agent *Pseudomonas fluorescens* CHA0. Journal of Bacteriology. 1998;**180**:3187-3196

[16] Kawakami R, Satomura T, Sakuraba H, Ohshima T. L-Proline dehydrogenases in hyperthermophilic archaea: Distribution, function, structure, and application. Applied Microbiology and Biotechnology. 2012;**93**:83-93. DOI: 10.1007/s00253-011-3682-8

[17] Ronchel MC, Ramos C, Jensen LB, Molin S, Ramos JL. Construction and behavior of biologically contained bacteria for environmental applications in bioremediation. Applied and Environmental Microbiology. 1995;**61**:2990-2994

[18] Tremblay G, Gagliardo R, Chilton WS, Dion P. Diversity among opine-utilizing bacteria: Identification of coryneform isolates. Applied and Environmental Microbiology. 1987;**53**:1519-1524

[19] Ogawa-Ohnishi M, Matsushita W, Matsubayashi Y. Identification of three hydroxyproline *O*-arabinosyltransferases in *Arabidopsis thaliana*. Nature Chemical Biology. 2013;**9**:726-730. DOI: 10.1038/nchembio.1351

[20] Fujita K, Takashi Y, Obuchi E, Kitahara K, Suganuma T. Characterization of a novel β-L-arabinofuranosidase in *Bifidobacterium longum*: Functional elucidation of a DUF1680 protein family member. Journal of Biological Chemistry. 2014;**289**:5240-5249. DOI: 10.1074/jbc.M113.528711

[21] Shibasaki T, Mori H, Chiba S, Ozaki A. Microbial proline 4-hydroxylase screening and gene cloning. Applied and Environmental Microbiology. 1999;**65**:4028-4031

[22] Bater AJ, Venables WA, Thomas S. Allohydroxy-D-proline dehydrogenase: An inducible membrane-bound enzyme in *Pseudomonas aeruginosa* PA01. Archives of Microbiology. 1977;**112**:287-289

[23] Kawakami R, Sakuraba H, Ohshima T. Gene and primary structures of dye-linked L-proline dehydrogenase from the hyperthermophilic archaeon *Thermococcus profundus* show the presence of a novel heterotetrameric amino acid dehydrogenase complex. Extremophiles. 2004;**8**:99-108. DOI: https://doi.org/10.1007/s00792-003-0368-x

[24] Tsuge H, Kawakami R, Sakuraba H, Ago H, Miyano M, Aki K, Katunuma N, Ohshima T. Crystal structure of a novel FAD-, FMN-, and ATP-containing L-proline dehydrogenase complex from *Pyrococcus horikoshii*. Journal of Biological Chemistry. 2005;**280**:31045-31049. DOI: 10.1074/jbc.C500234200

[25] Chen S, White CE, diCenzo GC, Zhang Y, Stogios PJ, Savchenko A, Finan TM. L-Hydroxyproline and D-proline catabolism in *Sinorhizobium meliloti*. Journal of Bacteriology. 2016;**198**:1171-1181. DOI: 10.1128/JB.00961-15

[26] Watanabe S, Tajima K, Fujii S, Fukumori F, Hara R, Fukuda R, Miyazaki M, Kino K, Watanabe Y. Functional characterization of aconitase X as a *cis*-3-hydroxy-L-proline dehydratase. Scientific Reports. 2016a;**6**:38720. DOI: 10.1038/srep38720

[27] Watanabe S, Tajima K, Matsui K, Watanabe Y. Characterization of iron-sulfur clusters in flavin-containing opine dehydrogenase. Bioscience, Biotechnology, and Biochemistry. 2016;**80**:2371-2375. DOI: 10.1080/09168451.2017.1403887

[28] Watanabe S, Tanimoto Y, Yamauchi S, Tozawa Y, Sawayama S, Watanabe Y. Identification and characterization of *trans*-3-hydroxy-L-proline dehydratase and Δ^1-pyrroline-2-carboxylate reductase involved in *trans*-3-hydroxy-L-proline metabolism of bacteria. FEBS Open Bio. 2014;**4**:240-250. DOI: 10.1016/j.fob.2014.02.010. eCollection 2014